JOURNAL OF MATERIALS SCIENCE 22 (1987) 2783–2788

Formation and growth of iron nitrides during ion-nitriding

E. METIN, O. T. INAL*
Materials and Metallurgical Engineering Department, New Mexico Institute of Mining and Technology, Socorro, New Mexico 87801, USA

In order to clarify the formation and growth kinetics of iron nitrides, Fe_2N (ξ), $Fe_{2-3}N$ (ε) and Fe_4N (γ'), on the surface of iron during ion-nitriding, and their contribution to the mechanism of ion-nitriding coarse-grained specimens (2 to 6 mm) were ion-nitrided in pure nitrogen and nitrogen–hydrogen (20%–80%) plasma at temperatures between 500 and 600° C. Reflection electron diffraction (RED) showed immediate formation of the nitrides. Growth of these phases in latter stages of ion-nitriding was studied using optical microscopy and X-ray diffraction. The mechanism of the nitride layer formation is discussed and compared with the existing gas nitriding data. In the case region, Fe_4N (γ') and $Fe_{16}N_2$ (α'') precipitation was observed to occur under all experimental conditions studied. Case depth is seen to be parabolic with time and nitriding rate increases slightly when nitrogen–hydrogen plasma is used. Discussions are given to explain the difference in the nitriding efficiency under two different plasma compositions.

1. Introduction

Ion-nitriding of steels has recently received considerable industrial interest due to the beneficial surface property enhancement when compared to other commercial nitriding processes. It is more economical and introduces faster nitrogen diffusion which in turn allows for lower nitriding temperatures or shorter treatment times. The process has been successfully applied to low alloy steels, tool steels, and stainless steels [1–3],

In the past decade several investigations have been conducted for the elucidation of the mechanism of ion-nitriding. Understanding of the actual mechanism of glow discharge surface hardening is rather crucial because it leads to the point of predicting the final properties of the nitrided components. Ionic bombardment, which introduces vacancies and vacancy clusters and therefore increases nitrogen diffusion, was thought to be singly responsible for this process [4–6]. Tibbetts [7] achieved nitriding with a positively biased grid above the sample and therefore claims that neutral atomic nitrogen is the main active species.

Another approach [7–9] considers the assumption of the formation of iron nitrides (FeN and Fe_2N) in the plasma. These nitrides, being unstable at nitriding temperatures, decompose to lower iron nitrides at the cathode surface and thus release free nitrogen to diffuse into the iron. As a part of the latter approach Rie and Lampe [10] introduced the concept of free energy of nitride formation to predict the dominating mechanism of ion-nitriding for non-ferrous metals. A major controversy emanates from the difference in the nitriding kinetics under different plasma compositions; mainly N–H containing plasma, nitrogen or nitrogen–argon plasma. The differences observed could not simply be explained by the reducing effect of hydrogen because both conditions have led to the formation of an Fe_4N layer on the surface [5, 8].

The purpose of this investigation was to study the formation and growth of iron nitrides on the surface of iron during ion-nitriding under two different plasma conditions and to elucidate their contribution to the actual mechanism of ion-nitriding. Reflection electron diffraction (RED) was utilized because this technique provides relatively small penetration depths (5 to 10 nm) and small sampling areas (20 to 100 μm) [11]. Optical metallography and X-ray diffraction techniques were also utilized to study the formation and growth of these nitrides.

2. Experimental procedure

2.1. Specimen preparation

Pure iron (> 99.85%) samples of 1 in. diameter and $\frac{1}{4}$ in. thick were vacuum annealed at 800° C for 5 h, to obtain relatively large, uniform grain size. The samples were polished through 3.0 μm alumina and cleaned in alcohol prior to ion-nitriding treatment.

2.2. Ion-nitriding

The ion-nitriding unit utilized in this study was similar to the system used in previous studies [1, 2, 12]. Ultra high purity (99.999%) hydrogen and nitrogen were used as discharge gases. Temperature was measured using a calibrated chromel alumel thermocouple embedded in the sample. All the experiments were

*Author to whom all correspondence should be addressed.

0022–2461/87 $03.00 + .12

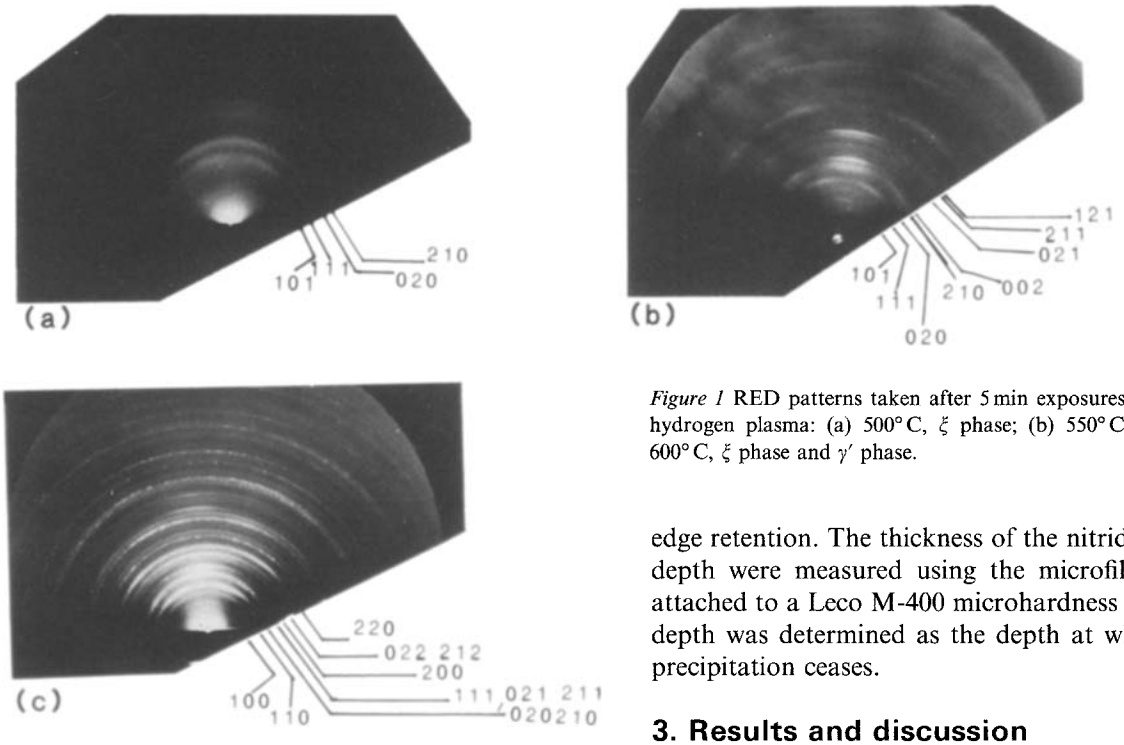

Figure 1 RED patterns taken after 5 min exposures to nitrogen–hydrogen plasma: (a) 500° C, ξ phase; (b) 550° C, ξ phase; (c) 600° C, ξ phase and γ' phase.

conducted at 10 torr total pressure measured with a barometrically compensated vacuum gauge.

2.3. Reflection electron diffraction and scanning electron microscopy

An RCA EMU-3G transmission electron microscope was equipped with an electron diffraction stage placed in the position of the intermediate lens. The microscope was operated at 100 kV and all diffraction patterns were taken immediately after the sample cooled down from the ion-nitriding temperature under vacuum. A Hitachi HHS-2R SEM, operated at 20 kV, was used to study the resulting surface morphologies.

2.4. X-ray diffraction and optical metallography

A Rigaku wide-range diffractometer was used for the X-ray diffraction analysis. The X-ray tube had a copper target and was operated at 40 kV, 25 mA with Cu$K\alpha$ radiation. The diffractometer was equipped with a wide-range goniometer and a scintillation counter. Specimens were scanned through 2θ values ranging from 20° to 95° at 1° min^{-1}.

The samples for optical microscopy were mounted in a metallic glass powder–epoxy medium to ensure edge retention. The thickness of the nitrides and case depth were measured using the microfilar eyepiece attached to a Leco M-400 microhardness tester. Case depth was determined as the depth at which nitride precipitation ceases.

3. Results and discussion

3.1. Surface studies

Fig. 1 shows the RED patterns obtained from samples which were exposed to nitrogen–hydrogen plasma for 5 min at temperatures between 500 and 600° C. The patterns taken at 500 and 550° C could be indexed to Fe_2N. Streaking in the diffraction patterns indicates a growth texture and the texture was also clear at later stages, as shown in Fig. 2. Ion-nitriding at 600° C for very short durations resulted in the formation of Fe_4N in addition to Fe_2N. The presence of the two phases together indicates the ξ-phase was either too thin or not continuous on the surface. X-ray diffraction analysis did not show any ξ-phase formation which also indicates that this phase is too thin to contribute to the diffraction (Table I). At temperatures above 550° C no ε-phase formation was observed in agreement with a previous observation [13].

In contrast to nitrogen–hydrogen plasma, pure nitrogen plasma did not exhibit ξ-phase formation (Fig. 3) possibly due either to the lower activation energy required to form this phase with the active ingredients of a nitrogen–hydrogen plasma or to the reduced stability of ξ-phase under pure nitrogen plasma that leads to an immediate decomposition.

Formation of these nitrides at the very early stages of ion-nitriding indicates that these nitrides were formed by sputtering of iron atoms from the cathode surface, forming the nitrides in the cathode fall space

TABLE I Phases identified using X-ray diffraction

Plasma	Temperature (° C)	Phases after:		
		0.5 h	2 h	6 h
Nitrogen	500	$\gamma' + \varepsilon + \alpha$	$\gamma' + \varepsilon$	$\gamma' + \varepsilon$
	550	$\gamma' + \varepsilon$	$\gamma' + \varepsilon$	$\gamma' + \varepsilon$
	600	$\gamma' + \alpha$	$\gamma' + \alpha$	$\gamma' + \alpha$
Nitrogen–hydrogen	500	$\gamma' + \alpha$	$\gamma' + \alpha$	$\gamma' + \alpha$
	550	$\gamma' + \alpha$	$\gamma' + \varepsilon + \alpha$	$\gamma' + \varepsilon + \alpha$
	600	$\gamma' + \alpha$	$\gamma' + \alpha$	$\gamma' + \alpha$

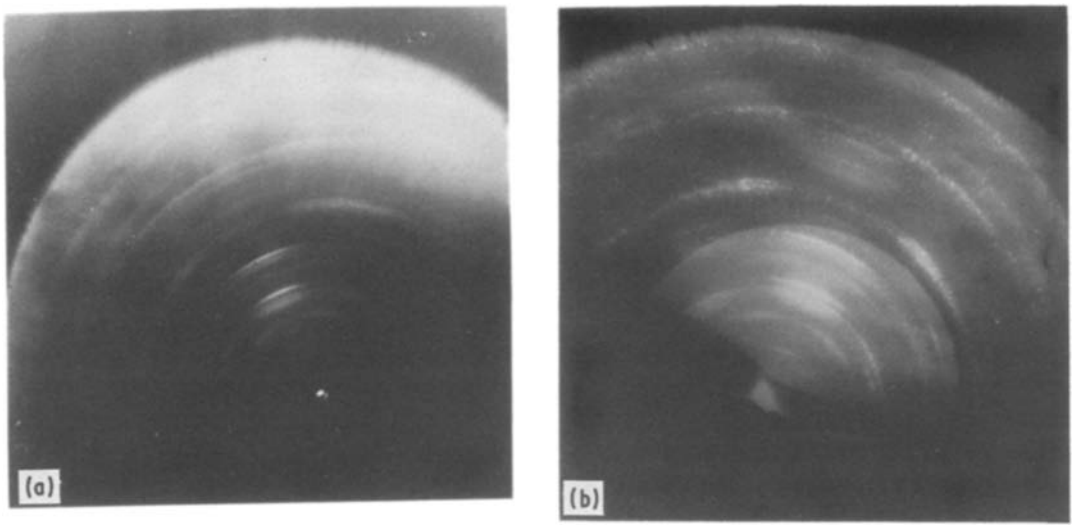

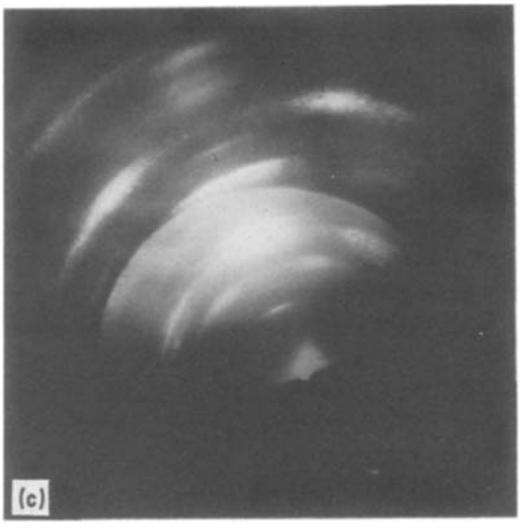

Figure 2 RED patterns obtained at later stages of ion-nitriding at 550° C, indexed to ξ phase: (a) 30 min; (b) 4 h; (c) 8 h.

and condensation to the cathode surface. High temperatures achieved in the plasma and the presence of nitride forming elements in the ionic or atomic form could have been sufficient to overcome the energy barrier to form these compounds. The present data seem to be first of their kind to give positive proof, in the form of electron diffraction patterns, for this long-standing hypothesis. Supporting evidence was also obtained from SEM analysis, as shown in Fig. 4, where the very small particles, of the order of a micrometre size, are clearly visible. These small particles suggest that nitrides are formed by a vapour deposition-like process.

A major difference between ion-nitriding and gas nitriding seems to be clarified by the present study by the observation of iron nitrides that are formed on the surface. Comparison of the surface micrographs of ammonia-nitrided iron [13, 14] with the present data shows that, during gas nitriding, nitrides are formed when the surface of iron has reached a saturation level for nitrogen, by a nucleation and growth mechanism. This would require an incubation period that may take from 20 to 120 min depending on the nitrogen partial pressure [14]. In the case of ion-nitriding the formation of iron nitrides, which produces a large concentration gradient on the surface, was immediate. This partially accounts for the discrepancy between the two processes.

Another important difference between the gas and ion nitriding, may be explained in terms of the possibility of enhanced nitrogen diffusion in the nitride layer due to ion bombardment during ion nitriding; even though the process must be considered in the low energy context. Because the nitride formation occurred immediately in the present study, it is not reasonable to expect any change in the nitrogen diffusivity in α iron due to ion bombardment (ion bombardment can only create damage within ~ 5 nm depth at this low energy level [15]. Previous investigation on the other hand, has shown that, even for very low average ion bombardment energies down to ~ 100 eV,

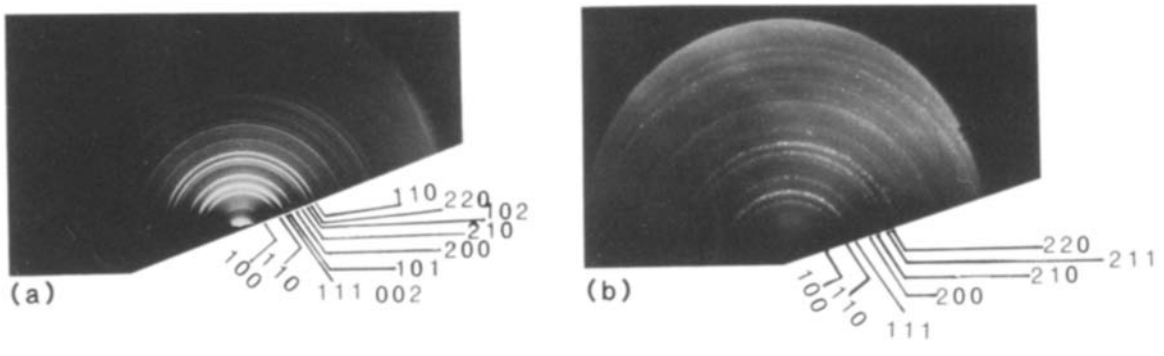

Figure 3 RED patterns taken after 5 min exposures to nitrogen plasma: (a) 550° C, γ' and ε phase; (b) 600° C, γ' phase.

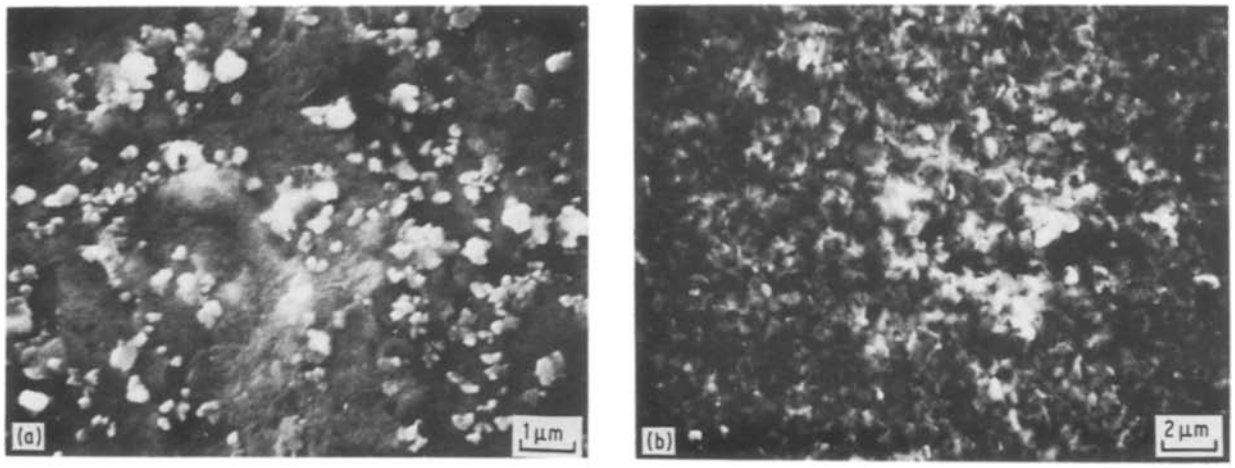

Figure 4 Scanning electron micrographs of the ion-nitrided surfaces, 550° C 5 min: (a) Nitrogen-hydrogen plasma; (b) nitrogen plasma.

enhancements in interfacial diffusion of up to 10^5 times over thermal values can be obtained, because of the excess defect density produced [15]. However, SEM analysis of the present study indicates that particles covering the surface are very small in size and that a short-circuit diffusion, through the boundaries in the nitride layer would very likely occur. As it is an established fact that grain boundary diffusion can be 10^9 times faster than that of the lattice diffusion [16] at low temperatures, grain-boundary diffusion in the nitride layer could also be an additional factor in increasing the nitriding kinetics.

Nitrogen diffusion in γ' is much slower than in α iron [17]. Therefore, the rate-limiting step is the nitrogen diffusion in the nitride layer which controls the total flux to the interface. The faster the nitrogen diffusion to the interface, the faster would be the nitriding reaction in iron. On the basis of these points, the major effect of ion bombardment is possibly its role in the nitride formation, as suggested earlier. The small grain size in the nitride layer together with the ion bombardment effect at the surface could produce faster diffusion in the nitride layer, therefore increasing the kinetics of nitriding in the iron. From this point of view a comparative diffusion analysis in the nitride layer could produce valuable information on the mechanism of ion-nitriding.

3.2. Growth of surface nitrides

The growth kinetics of iron nitrides were studied using optical metallography. The thickness of the nitride layers as a function of time is given in Figs 5 and 6 at two different plasma compositions. The growth of the nitride layer is not parabolic with time at least at the initial stages of ion nitriding as opposed to observations in gas nitriding [17]. An initial increase in the thickness of the nitride layer is seen to be followed by a region in which the thickness of the nitride layer is hardly effected by time. This can be explained in terms of the quantity of iron atoms sputtered from the cathode surface. Initially iron concentration at the surface is higher and therefore the mean free path of iron atoms in the plasma would be lower, yielding a higher rate of nitride formation. Increasing time of ion nitriding would cause a decrease in iron concentration at the surface, due to the complete coverage of the surface with iron nitrides and, therefore, the mean free path of iron atoms would be larger. This, in turn, causes a lower rate of nitride formation. In Fig. 5 the growth rate of the nitride layer for ammonia-nitrided iron taken from Schwerdtfeger *et al.* [17] is also shown for comparison. It is apparent from this that initially ion-nitriding produces thicker nitride layers, whereas extrapolation of data to longer times shows that ammonia nitriding produces thicker nitride layers. The thickness of the nitride layer, in pure nitrogen, was observed to be slightly thicker than the nitride layer obtained in nitrogen–hydrogen plasma, possibly due to the change in nitrogen partial pressure.

3.3. Characterization of the diffusion zone

The diffusion zone of ion-nitrided iron was observed to be decorated with Fe_4N and $\alpha''(Fe_{16}N_2)$ precipitates as shown in Fig. 7. Large disc-shaped platelets of Fe_4N precipitated from the supersaturated α-matrix and are seen to lie parallel to the $\{2\,1\,0\}$ planes in

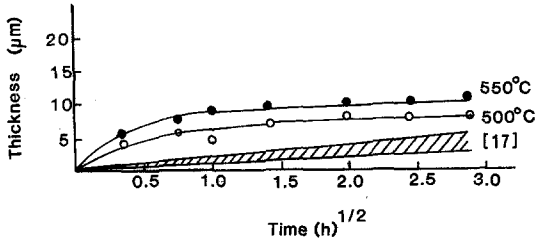

Figure 5 Thickness of the nitride layer as a function of time nitrogen-hydrogen plasma). The shaded area represents the growth of Fe_4N in ammonia nitrided iron with 29.2–53.3% NH_3 [17].

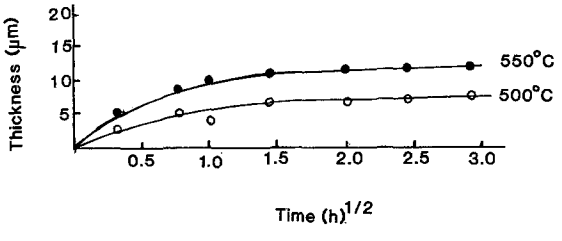

Figure 6 Thickness of the nitride layer as a function of time obtained by using nitrogen plasma.

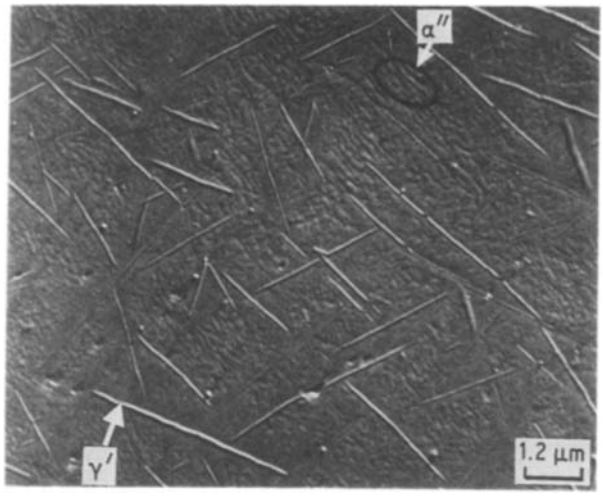

Figure 7 Electron micrographs of a typical case region showing α'' ($Fe_{16}N_2$) and γ' (Fe_4N) precipitation.

the α-matrix [18]. The transition nitride, α'', has been first observed to occur, as a precursor to the Fe_4N during tempering of nitrogen martensite [19]. These precipitates were observed to have a preferred orientation with the matrix, orientation being a function of the sign of diffusion-induced stresses [20]. Both types of precipitations were observed to occur independent of plasma composition used.

Interstitial nitrogen stabilizes the γ phase at temperatures above 590° C. During cooling from these temperatures this phase decomposes to γ' and α as dictated by the Fe–N phase diagram. The decomposed austenite is shown in Fig. 8 and the growth of this phase is shown in Fig. 9. The rate is parabolic with time and the small difference in growth kinetics with the two types of plasmas studied seems to be within experimental error.

Fig. 10 shows the case depths as functions of time for both plasmas studied. Case growth is parabolic with time for both plasmas which indicates a volume diffusion-controlled process, being faster with nitrogen-hydrogen plasma. The activation energy for a diffusion-controlled growth is given by [21];

$$d\xi^2/dt = A \exp(-Q/RT) \quad (1)$$

where $d\xi^2/dt$ is the slope of the case depth against time relationship, A is the linear rate constant, Q is the activation energy for the process, R is the gas constant and T is the absolute temperature. The application of this equation is presented in Fig. 11. However, the application of this equation requires the process to be totally diffusion controlled. It was previously shown (Figs. 5 and 6) that the growth of the nitride layer is not parabolic. Therefore, the resulting activation energies using Equation 1 will not necessarily be the activation energy for nitrogen diffusion in α iron, although the growth of this layer is controlled by nitrogen diffusion, but the activation energy for the process which can only be used under identical conditions. Comparison of the calculated values (Q = 12 750 cal mol^{-1} for nitrogen-hydrogen plasma and Q = 14 170 cal mol^{-1} for nitrogen plasma) with the activation energy for nitrogen diffusion (Q = 17 540 cal mol^{-1}) [22] will therefore be a direct indication of faster kinetics induced by ion-nitriding.

A possible explanation for the faster nitriding with nitrogen–hydrogen plasma may be due to the lack of ξ phase formation with nitrogen plasma. This could be directly related to the non-equilibrium state of the plasma, the energy transfer between the gas–solid interface, and the chemical reactivity of the surface with the nitriding plasma as pointed out in earlier investigations [23].

4. Conclusions

1. The mechanism of ion-nitriding involves the formation of ξ (Fe_2N) phase at the surface, at the very early stages of ion-nitriding, though some reactions were improved by sputtering processes. Nitriding reaction continues with further decomposition of ξ to γ' (Fe_4N) or ε ($Fe_{2-3}N$) depending on the temperature.

2. Immediate formation of these nitrides at the surface, which builds up a large concentration gradient and possibly faster diffusion in the nitride layer due to small grain size, was thought to be the basic reason behind the superiority of ion-nitriding over other commercial techniques. Free nitrogen supplied by the decomposition of ξ phase may also be a contributing factor, as pointed out by Edenhofer [8].

3. The thickness of the nitride layer obtained under pure nitrogen plasma is slightly larger than that of nitrogen–hydrogen plasma. The growth of the nitride layers obtained under both plasma compositions studied was not parabolic with time, at least for the initial stages.

4. Extensive precipitations in the case regions were

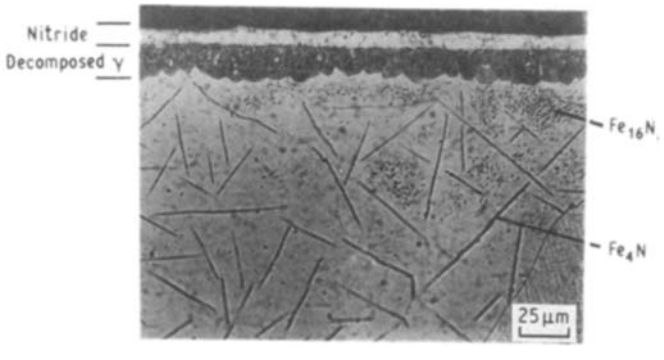

Figure 8 Optical micrographs showing the cross-section of ion-nitrided iron at 600° C.

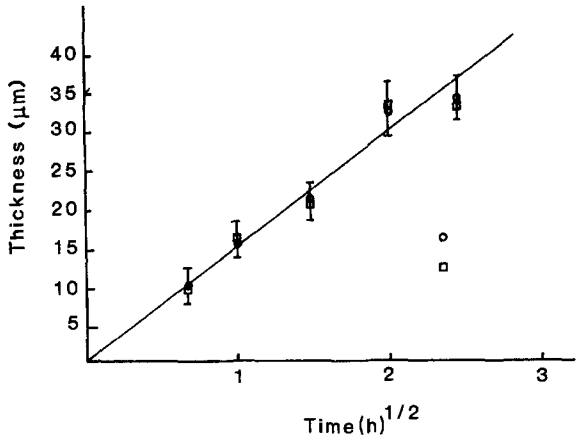

Figure 9 Thickness of the decomposed γ as a function of time using (□) nitrogen and (○) nitrogen-hydrogen plasma; $T = 600°C$.

observed to occur in the form of large platelets of Fe_4N and oriented platelets of $Fe_{16}N_2$.

5. Nitrogen–hydrogen mixture produced larger case depths than pure nitrogen, possibly due to absence of ξ-phase formation. Case depth in both cases was parabolic with time which indicates a volume diffusion-controlled process.

6. Activation energies calculated for the case growth yield lower values than the activation energy required for nitrogen diffusion in α iron. The difference is assumed to be due to non-parabolic growth of the nitride layer which limits the applicability of the equations utilized and therefore is accepted as a direct indication of the faster kinetics of nitriding induced by ion-nitriding.

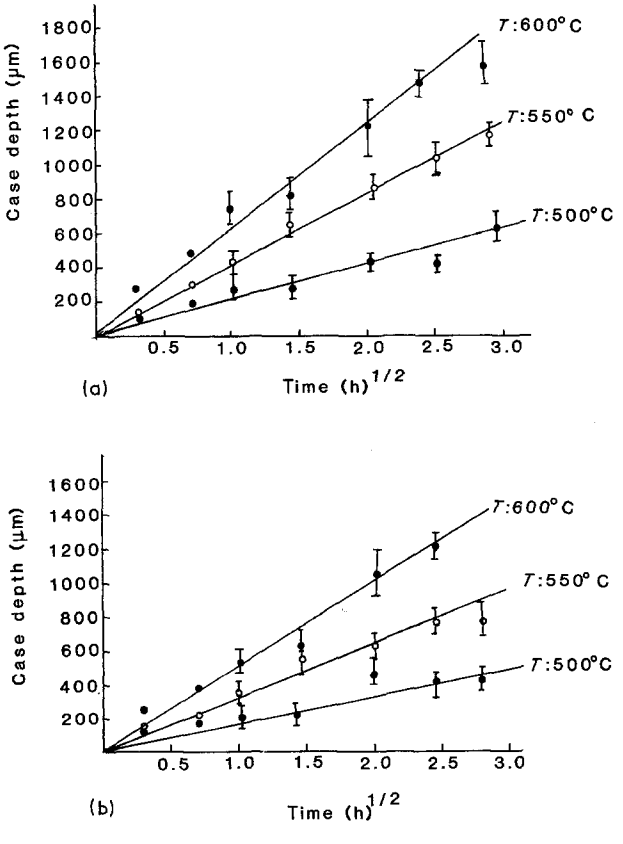

Figure 10 Case depth as a function of time, (a) nitrogen–hydrogen plasma; (b) nitrogen plasma.

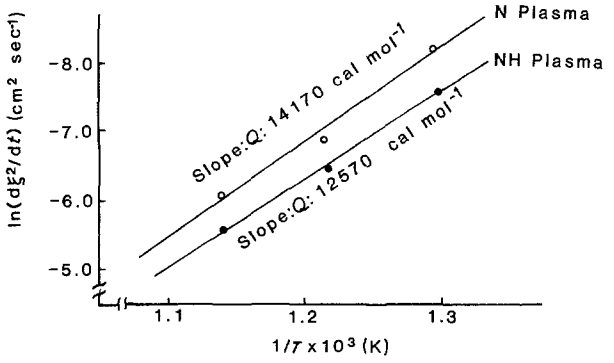

Figure 11 Logarithm of the rate constant as a function of the reciprocal temperature for nitrogen–hydrogen plasma and nitrogen plasma nitrided iron.

Acknowledgements

Financial support for this research supplied by Research and Development Division of New Mexico Institute of Mining and Technology and New Mexico Chapter of American Vacuum Society in the form of a scholarship given to Mr E. Metin is gratefully appreciated.

References

1. C. V. ROBINO and O. T. INAL, *Mater. Sci. Eng.* **59** (1982) 79.
2. K. OZBAYSAL, O. T. INAL and A. D. ROMIG, *ibid.* **78** (1986) 179.
3. K. OZBAYSAL and O. T. INAL, *J. Mater. Sci.* **21** (1986) 4318.
4. H. STRACK, *J. Appl. Phys.* **34** (1963) 2405.
5. M. HUDIS, *ibid.* **44** (1973) 1489.
6. A. V. BROKMAN and R. F. TULER, *ibid.* **52** (1981) 468.
7. G. G. TIBBETTS, *ibid.* **45** (1974) 5072.
8. B. EDENHOFER, *Heat Treat. Met.* **1** (1974) 23.
9. YU. M. LAKHTIN, YA. D. KOGAN and V. N. SHAPOSHNIKOV, *Metall. Term. Obrabotka Metallov* **6** (1976) p. 2.
10. K. T. RIE and TH. LAMPE, *Mater. Sci. Eng.* **69** (1985) 475.
11. A. SCHERER and O. T. INAL, *Thin Solid Films* **119** (1984) 413.
12. O. T. INAL and C. V. ROBINO, *ibid.* **95** (1982) 195.
13. Y. INOKUTI, N. NISHIDA and N. OHASHI, "Source book on nitriding" (ASM, 1977) p. 303.
14. H. C. F. ROZENDAAL, E. J. MITTEMEIJER, P. F. COLIJN and P. J. VAN DER SCHAAF, *Metal. Trans. A* **14A** (1983) 395.
15. A. H. ETOUKHY and J. E. GREENE, *J. Appl. Phys.* **51** (1980) 4444.
16. A. R. WAZZAN, *ibid.* **36** (1965) 3596.
17. K. SCHWERDTFEGER, P. GRIEVESON and E. T. TURKDOGAN, *Trans. AIME* **245** (1969) 2461.
18. R. F. MEHL, C. S. BARRETT and H. S. JERABEK, *ibid.* **113** (1934) 211.
19. K. H. JACK, *Proc. R. Soc.* **A208** (1951) 216.
20. W. T. M. STRAVER, H. C. F. ROZENDAAL and E. J. MITTEMEIJER, *Met. Trans. A* **15A** (1984) 627.
21. J. W. CHRISTIAN, "Transformations in Metals and Alloys" (Pergamon Oxford, 1975).
22. J. R. G. DA SILVA and REX B. McLELLAN, *Mater. Sci. Eng.* **26** (1976) 83.
23. A. GICQUEL, M. P. BERGOUGNAN, J. AMOUROUX and D. RAPAKOULIAS, "Plasma chemistry and technology", Proceedings of the Conference, San Diego, California (1982) p. 159.

Received 1 August
and accepted 25 November 1986